Ultra-Low Shrinkage Hybrid Photosensitive Material for Two-Photon Polymerization Microfabrication

Aleksandr Ovsianikov,[†] Jacques Viertl,[†] Boris Chichkov,[†,§,*] Mohamed Oubaha,[‡] Brian MacCraith,[‡] Ioanna Sakellari,[§,⊥] Anastasia Giakoumaki,[§,¶] David Gray,[§] Maria Vamvakaki,[§,¶] Maria Farsari,[§] and Costas Fotakis[§,⊥]

[†]Nanotechnology Department, Laser Zentrum Hannover e.V., 30419, Hannover, Germany, [‡]Optical Sensors Laboratory/National Centre for Sensor Research, Dublin City University, [§]Institute of Electronic Structure and Laser (IESL), Foundation for Research and Technology Hellas (FORTH), [⊥]Department of Physics, University of Crete, and [¶]Department of Materials Science and Technology, University of Crete

ABSTRACT Investigations into the structuring by two-photon polymerization of a nonshrinking, photosensitive, zirconium sol—gel material are presented. This hybrid material can be photostructured even when it contains up to 30 mol % of zirconium propoxide (ZPO); by varying the material's inorganic content, it is possible to modify and tune its refractive index. The introduction of ZPO significantly increases the photosensitivity of the resulting photopolymer. The fabricated three-dimensional photonic crystal structures demonstrate high resolution and a clear band-stop in the near-IR region. In contrast to common practice, no additional effort is required to precompensate for shrinkage or to improve the structural stability of the fabricated photonic crystals; this, combined with the possibility of tuning this material's optical, mechanical, and chemical properties, makes it suitable for a variety of applications by two-photon polymerization manufacturing.

KEYWORDS: hybrid materials · nonlinear optics · photochemistry · polymeric materials · photonic crystals

Since the introduction of the principle of the photonic band gap, the design and construction of three-dimensional (3D) photonic crystal devices has been the subject of intensive research.[1−3] However, the fabrication of such devices, operating in the visible range, is still a major technological issue.

Nonlinear optical microstructuring, a technique based on two-photon polymerization of organic materials, allows the fabrication of 3D structures with high resolution. When the beam of an ultrafast infrared laser is tightly focused into the volume of a photosensitive material, the polymerization process can be initiated by two-photon absorption within the focal volume. By moving the laser focus three-dimensionally through the resin, 3D structures can be fabricated. The technique has been used with several acrylate and epoxy materials, and complex 3D components and devices have been fabricated, such as mechanical devices and microscopic models.[4,5] Resolution below 100 nm has been achieved using this technique.[6]

The fabrication of 3D photonic crystals by two-photon polymerization (2PP) has been researched extensively by several groups.[7,8] Much of this research has concentrated on the fabrication of photonic crystals with complete band gaps located in the near-IR region, at the telecommunication wavelengths—a challenging task, as the structural resolution of such photonic crystals approaches the limit of resolution of the technology and the employed materials. A further shift of the band gaps' central frequency into the visible ranges requires further downscaling of the structures and imposes an even bigger challenge on the current fabrication approaches and employed materials. Commonly used photosensitive materials exhibit shrinkage, which can lead to the distortion of the fabricated crystals and the disappearance of the photonic band gap. In order to avoid such distortions, the structure can be numerically precompensated or mechanically stabilized by providing a solid support frame around it.[3,9]

Sol−gel organic−inorganic hybrid technology provides a very powerful tool for the development of photosensitive materials. Sol−gel materials benefit from straightforward preparation, modification, and processing, and in combination with their high optical quality, postprocessing chemical and electrochemical inertness, good mechanical and chemical stability, they have found several applications in photonic devices such as photonic crystals and waveguides.[10−14] The copolymerization of a silicon alkoxide with a zirconium alkoxide

*Address correspondence to b.chichkov@lzh.de.

Received for review July 18, 2008 and accepted October 21, 2008.

Published online November 1, 2008.
10.1021/nn800451w CCC: $40.75

© 2008 American Chemical Society

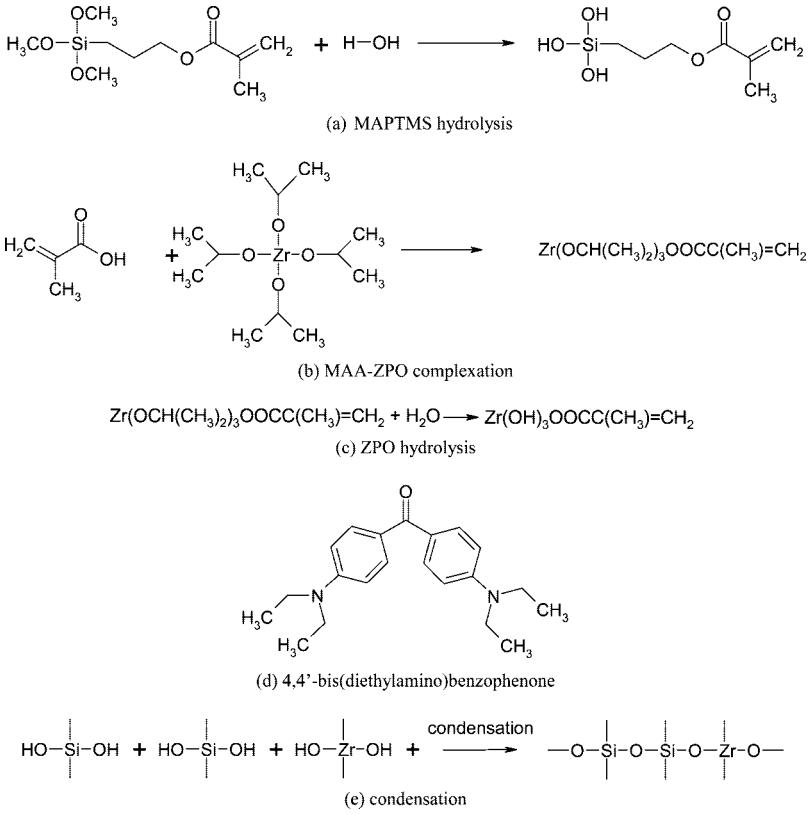

Figure 1. Chemical structures of the reagents and sol−gel process leading to the formation of the inorganic matrix.

has been shown to enhance the material's mechanical stability and allow the modification of its refractive index.[15,16] Sol−gel materials provide the possibility of the incorporation of various functional groups by using a guest−host or a side-chain−main-chain strategy. One example is the incorporation of a nonlinear optical chromophore to produce an electro-optically active sol−gel. Planar devices made of such materials have been extensively studied.[17,18] Similar sol−gel systems have been used for 3D lithography[19] previous to this work.

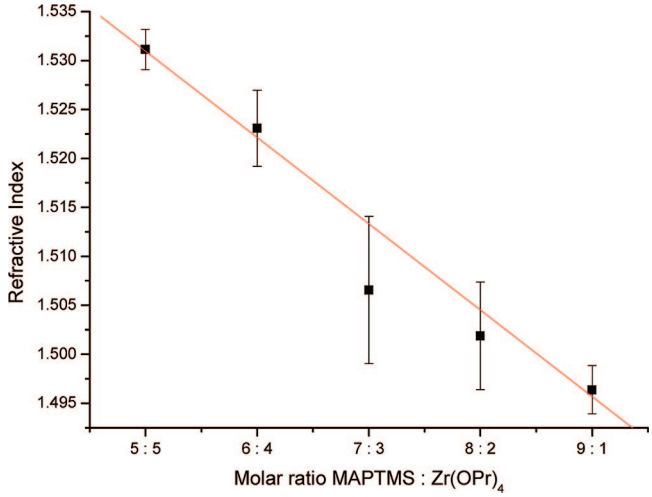

Figure 2. Refractive index of the material as a function of ZPO content at 632.8 nm.

In this work, we present our investigation into the fabrication of 3D photonic crystals by 2PP on a zirconium propoxide sol−gel. We show that, by organically modifying zirconium *n*-propoxide only partially, structure distortion due to shrinkage during photopolymerization can be avoided; this eliminates the need for design compensation or mechanical support for the structure. We also show that, the addition of zirconium *n*-propoxide significantly increases the photosensitivity of the photopolymer and that by varying the inorganic content of the sol−gel, the material refractive index can be tuned.

RESULTS AND DISCUSSION

The two main components of the copolymer employed in this work are methacryloxypropyl trimethoxysilane (MAPTMS) and ZPO. By varying the molar ratio of these, the refractive index of the composite can be modified, as shown in Figure 2. It can be seen that as the ZPO content increases, so does the material's refractive index. The fact that this increase is linear greatly simplifies the material design criteria, as typically such increases are saturating so that the doping concentration becomes very critical. However, in this concentration range, no such limitation is apparent.

Figure 3 shows the UV−visible absorption of thin films prepared from materials containing 0 and 30% ZPO, with addition of 1 and 0% 4,4′-bis(diethylamino) benzophenone photoinitiator (PI), respectively. The PI-free material does not show any absorption, while the material containing 1% PI shows a strong absorption centered at 365 nm. From these spectra, it is clear that the predominant absorption in the considered spectral range is ascribable to the PI.

Figure 4 shows the UV−visible absorption spectra of both liquids and thin films prepared from materials containing 5 and 30% ZPO, to which 1% of PI was added. It is observed that for both liquid and solid samples the increase of the zirconium concentration provokes a significant decrease of the absorption band located in the spectral range of 300−400 nm. However, in the solid state, an additional absorption band appears in the spectral range of 450−500 nm. The intensity of this band increases with the increase of the zirconium content, as also reported by Bhuian *et al.*, indicating an interaction between the ZPO and the PI.[12] In addition, a shift of this absorption peak maximum to the longer wavelength is clearly evidenced. This second peak disappears when the material is dissolved (Figure 3, solution curves), indicating that molecular proximity is required.

This effect could be ascribed to an electron transfer mechanism between the organic photoinitiator and the zirconium atoms and/or the formation of Zr−PI complexes due to the free d orbitals of the zirconium atoms. A most plausible explanation for the observed phenomenon could associate all these properties. In the solid state, the electrophilic zirconium atoms will tend to approach the electron-donating amino groups of the PI resulting in a close proximity and the formation of coordinated metal−ligand complexes. To the best of our knowledge, this is the first study that highlights such a bathochromic effect of the zirconium atom in the presence of PI. This phenomenon is critical as it governs the photosensitive properties of the PI and affects the fabrication process of photonic devices, especially for industrial applications. However, a more detailed investigation is required to verify the origin of this effect, which is out of the scope of the present work.

In order to study the influence of the ZPO content on the copolymer's structural resolution, 3.6 μm long free-hanging lines were fabricated, as shown in the inset of Figure 5. The dependence of the structure size on the average laser power at a constant scanning velocity is shown in Figure 5. For an average laser power of 22 mW, the voxel height tripled even when only 1% molar content of the chelated ZPO compound was added to the material. When no ZPO was added to the material mixture, no lines would survive the development process for an average power below 22 mW. A further increase of the ZPO content leads to a linear increase of the material sensitivity.

The average power is measured before the scanning unit, so after losses at the mirrors and the truncation by the microscope objective aperture, only 15% of laser power reaches the sample.

The inset in Figure 6 shows the side and top view of one of the fabricated woodpile photonic crystal structures exhibiting a band-stop in the near-IR region; in this case, the employed material had a 2:8 ZPO/MAPTMS molar ratio. As the material exhibits negligible distortion due to photopolymerization, no additional effort, such as precompensation or mechanical stabilization to avoid structural distortions, are necessary. All woodpiles were fabricated at scanning speed of 200 μm/s, the used laser power was in the range of 8−12mW adjusted so the dielectric filling fraction is approximately 50% for all structures. The rod cross-section height to width ratio is in direct relation to the used power varying in the range of 2.5−3.1. The interlayer distance was chosen such that the unit cell "width to height" ratio is preserved for all structures with the value of around 1.2. Fourier transform infrared spectroscopy (FTIR, Bruker Optics, Equinox) measurements of the reflection and the transmission spectra of woodpile structures with rod distances between 1.2 and 1.8 μm are shown in Figure 6. In accordance to Maxwell scaling, the central frequency of a band-stop is shifting

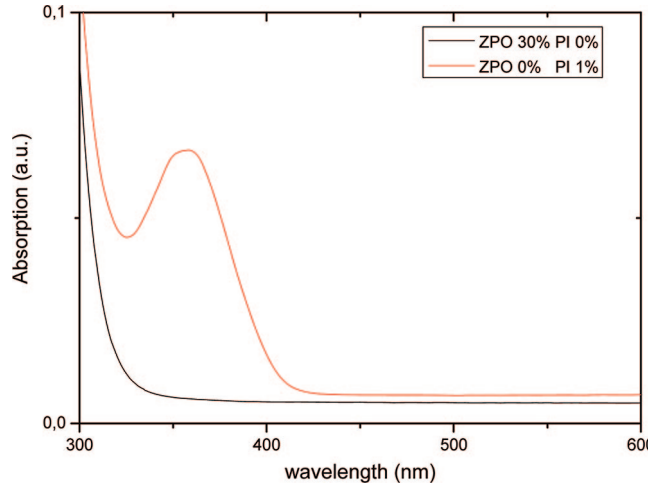

Figure 3. Transmission spectra of MAPTMS:ZPO and MAPTMS:PI thin films.

to shorter wavelengths as the unit cell size is reduced. The transmission suppression of up to 60% is achieved in fabricated structures. Since the reflection peak measurement is much more sensitive to scattering inside the photonic crystal and on the woodpile−glass/woodpile−air interfaces, the reflection peak amplitudes do not exceed 20%. In addition, the spectra show the appearance of higher order bandstops in all samples, indicating the high quality of the fabricated structures. There are two additional bands at 3 and 3.4 μm whose origin is the absorption of the material, as confirmed by measurements of transmission through flat, unstructured layers. As seen, the material has no natural absorption in the spectral region of 550−2700 nm, which makes it suitable for structuring by 2PP using a 780 nm laser, and for making photonic crystal structures at telecommunication wavelengths.

The observed splitting of the absorption and transmission peaks (*e.g.*, for the period of 1.6 μm, this splitting occurs around 2.4 μm) can be explained by taking a closer look at the experimental setup used for the FTIR transmission measurements. In order to focus the beam to the size of the fabricated photonic crystal, a Cassegrain reflective optical assembly is used. In contrast to

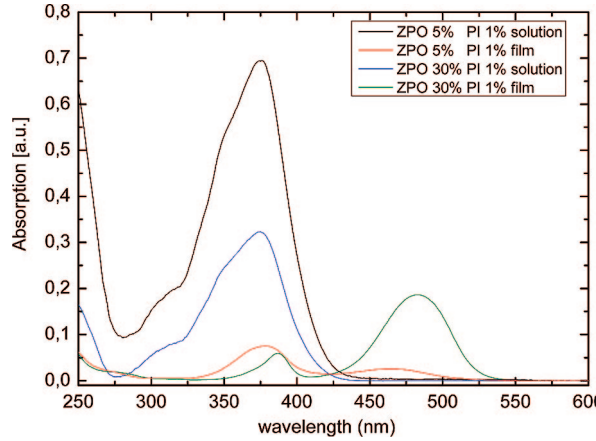

Figure 4. ZPO:MAPTMS:PI spectra in film and solution.

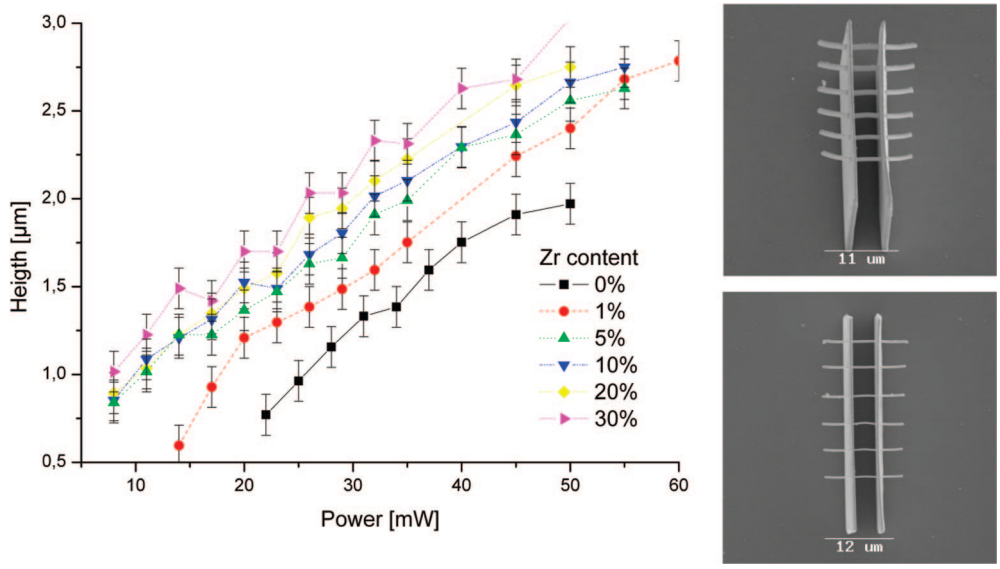

Figure 5. Voxel height dependence on the average laser power in relation to the ZPO content in the material (photoinitiator content is kept at a constant level of 1%). A constant scanning speed of 200 µm/s was used for all the structures. The inset shows the SEM images of examples of the structures used for free-hanging line height analysis.

the ideal case, when the measuring beam is perpendicular to the surface of the structure, this assembly provides illumination of the structure with a hollow light cone having an acceptance angle between 15 and 30°. Previous studies on 3D photonic crystal systems have shown that scattering of the measuring beam entering the photonic crystal at a large angle leads to the reflection peak splitting and a blue shift of its central position.[24,25] Theoretical simulations have also confirmed these observations.[26]

The majority of materials used in 2PP applications with free-radical polymerization are viscous liquids. The zirconium-containing material employed in this work, however, is a gel; this improves processability. In comparison to the SU8, which is another solid material used in 2PP microfabrication, the presented hybrid is marked by the straightforward preparation and postprocessing protocol. The overall sample processing times are also greatly reduced. Its real advantage over other 2PP materials derives, however, from its negligible shrinkage (see examples shown in Figure 7), due to its high cohesion at the molecular level. This molecular cohesion is intimately linked to the double polymerization ability of sol−gels. First, the mineral hydrolysis and condensation that occurs during the sol−gel synthesis allows the formation of polycondensable M−OH (M = Si, Zr) groups capable of forming strong covalent Si−O−Si, Zr−O−Zr, and Si−O−Zr bonds. After mixing the two monomer solutions, MAPTMS and MAA-Zr, in the third step, a condensation of the hydroxyl mineral groups takes place to form an in-

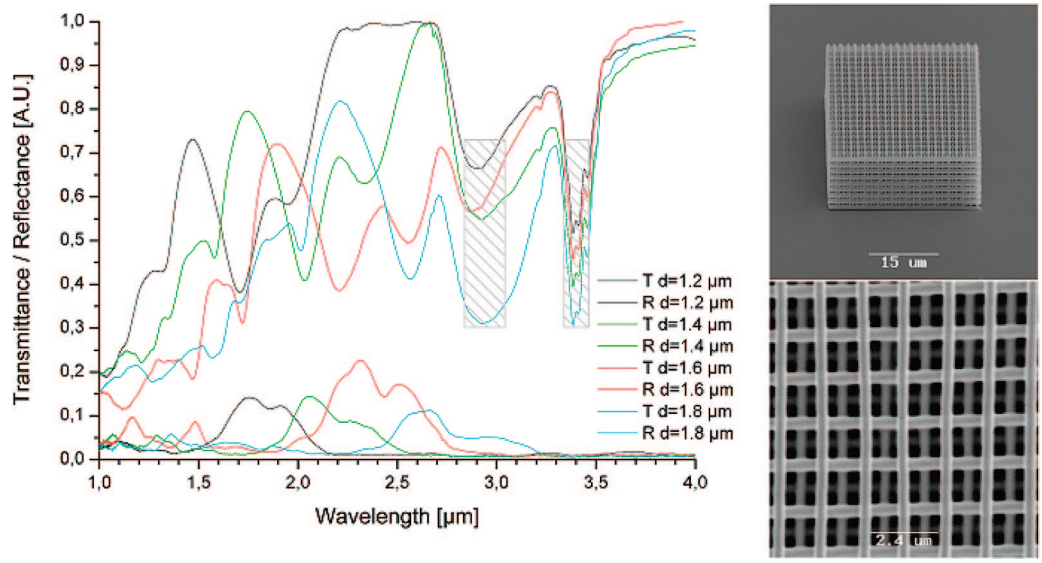

Figure 6. Transmittance and reflectance spectra of woodpile photonic crystal structures with different structure period d, varying between 1.8 and 1.2 µm. The absorption bands, indicated by gray rectangles, result from the material absorption. The inset shows the SEM side/top view images of a woodpile photonic crystal structure.

organic matrix with M−O−M moieties. The formation of these bonds is irreversible, as previously described.[27] During sample drying, alcohol, water, and any other solvents present in the film are released from the system and the unstructured material shrinks. This procedure results in the formation of a soft glass matrix onto which there are covalently attached organic methacrylate groups. The final step involves the photocopolymerization of the MAPTMS and MAA monomers. The organic groups attached to the inorganic backbone are polymerized using two photon polymerization with the aid of the photoinitiator by the formation of irreversible and fully saturated aliphatic C−C covalent bonds that further increase the connectivity of the material. At this stage, when the 3D structures are formed, the photoinitiated reaction results in linking together the pendant methacrylate groups of the system without the release of any molecules, and thus no significant distortion of the structures due to shrinkage is observed. The combination of the sol−gel condensation and the effect of irradiation produce a nonshrinkable material, the structure of which could be described as an organic skeleton rigidified by strong mineral bonds at its ends and makes it an ideal candidate for the fabrication of 3D structures.

An approach taken by many groups is the templating of photonic crystals by inversion, infiltrating them with another, higher refractive index material.[8,18] The materials described here can also be used for template fabrication. Like most hybrids, their organic components decompose at relatively low temperatures (approximately 220 °C). Therefore such processes like CVD or annealing of the structures will cause deformations. Increasing the ratio of the inorganic component was reported to result in less deformation of the annealed structures.[28] The inorganic components, however, which are dominant after condensation in the materials described here, are very resistant to high temperatures and chemicals.

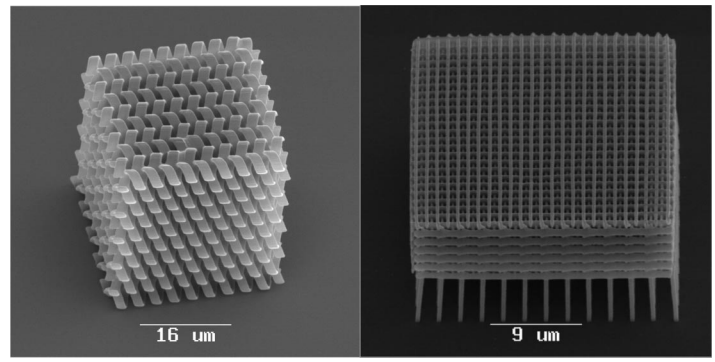

Figure 7. Three-dimensional photonic crystal structures produced by the 2PP technique.

METHODS

Materials. Methacryloxypropyl trimethoxysilane (MAPTMS, 99%, Polysciences Inc.) and methacrylic acid (MAA, >98%, Sigma-Aldrich) were used as the organic photopolymerizable monomers. Zirconium *n*-propoxide (ZPO, 70% in propanol, Sigma-Aldrich) and the alkoxysilane groups of MAPTMS served as the inorganic network forming moieties.

The difference in reactivity of the alkoxysilane and the zirconium precursor required a three-step procedure for the successful formation of the combined inorganic network: (1) MAPTMS and ZPO were separately hydrolyzed and stabilized by MAA, respectively (Figure 1a,b); (2) the prehydrolyzed MAPTMS was slowly added to the zirconate complex; and (3) final hydrolysis of the mixture was carried out (Figure 1c).

The hydrolysis of MAPTMS was performed using HCl solution (0.01 M) at a 1:0.75 ratio. Since MAPTMS is not miscible with water, the hydrolysis was carried out in a heterogeneous phase. However, after 20 min of stirring, the production of methanol and the hydrolysis of the alkoxysilane groups were sufficient to allow the miscibility of all species present in solution.

Strong complexing ligands have often been used in order to control the relative hydrolysis and condensation reaction rates of non-silicate metal alkoxide precursors. MAA has been employed as such a ligand and was shown to be covalently bound to the zirconium atom through its carboxy group. In our synthesis, MAA was added dropwise to the ZPO solution at a 1:1 MAA/Zr molar ratio. MAA reacted with ZPO to form a modified $Zr(OC_3H_7)_{4-x}(MAA)_x$ complex. Due to the equimolar proportions of metal alkoxide and MAA used in this preparation, the most probable resulting complex is $Zr(OC_3H_7)_3MAA$.

After 45 min, the partially hydrolyzed MAPTMS was slowly added to the zirconate complex. The molar ratio of MAPTMS to ZPO was varied from 10:0 to 5:5, in order to investigate the processability and the refractive index variation of the resulting gel. Following another 45 min, water was added to this mixture with a final 2.5:5 MAPTMS/H_2O molar ratio.

Finally, the photoinitiator (PI) 4,4′-bis(diethylamino) benzophenone (Sigma-Aldrich) (Figure 1d), at a 1% w/w concentration to the final material, was added to each mixture. After stirring for 24 h, the materials were filtered using 0.22 μm syringe filters.

The samples were prepared by spin-coating or drop-casting onto glass substrates, and the resultant films were dried on a hotplate at 100 °C for 1 h before the photopolymerization. The heating process resulted in the condensation of the hydroxy mineral moieties and the formation of the inorganic matrix (Figure 1e).

Refractive Index Measurements. The refractive index of the sol−gel films at 632.8 nm was determined from an m-line prism coupling experiment, using a He−Ne laser.[20] A thin film of the material was first made by spin-coating and subsequent curing under a UV lamp. A Schott Glass SF6 prism, as a higher refractive index medium, was used to couple light into the TE modes of the material waveguide; the sample was then mounted on a high-resolution rotation stage. The laser beam was directed toward the sample, and the transmitted light was detected with a photodiode. The coupling angles were then determined, and from the prism angle and refractive index, the mode indices of the modes could then be determined. From the crossing point of the modes supported by the thin film, both the thickness and the refractive index of the film could be then calculated from the mode equation.[19,20]

Transmission Spectra. The transmission spectra of both liquids and thin films samples were recorded in the 250−1100 nm spectral range using a Perkin-Elmer UV−vis spectrometer. Thin films were prepared by spin-coating the solutions and after drying on a hotplate at 100 °C for 1 h, and curing using a UV lamp.

Fabrication Using Two-Photon Polymerization. Two-photon polymerization is a direct laser writing technique, which allows the fabrication of complex 3D structures with a resolution below 100 nm.[21,22] In the present work, a Ti:sapphire laser (Chameleon, Coherent) delivering pulses of 140 fs duration at a repetition rate of 80 MHz and a central emission wavelength of 780 nm was

used. A 100× microscope objective lens (Zeiss, Plan Apochromat, N.A. = 1.4) was used to focus the laser beam into the volume of the photosensitive material. The complete experimental setup and procedure has been described elsewhere.[23] The employed material is transparent in the used near-infrared laser radiation; therefore, only two-photon absorption can initiate a photopolymerization process. Due to the threshold behavior and nonlinear nature of the 2PP process, the light−material interaction region is confined to the small volume within the focus of the laser beam. Resolution beyond the diffraction limit can be realized by controlling the laser pulse energy and the number of applied pulses. In this step, the final organic−inorganic network is formed by polymerizing the pendant methacrylate moieties. The material is polymerized along the trace of the moving laser focus, thus enabling fabrication of any desired polymeric 3D pattern by direct "recording" into the volume of a photosensitive material. In a subsequent processing step, the material, which was not exposed to the laser radiation, is removed by etching in propanol (Sigma-Aldrich) and the fabricated structure is revealed.

Acknowledgment. The authors would like to thank the group of Prof. Martin Wegener from Karlsruhe for providing access to FTIR equipment and fruitful scientific discussions. This work has been supported by the DFG "Photonic crystals" research program SPP1113, by the DFG "Rebirth" Excellence Cluster, by the Marie Curie Transfer of Knowledge project "NOLIMBA" (MTKD-CT-2005−029194), and by the UV Laser Facility operating at IESL-FORTH under the European Commission "Improving Human Research Potential" program (RII3-CT-2003−506350). Travel between Crete, Greece, and Hannover, Germany, was supported by an IKYDA/DAAD travel grant.

REFERENCES AND NOTES

1. Yablonovitch, E. Inhibited Spontaneous Emission in Solid-State Physics and Electronics. *Phys. Rev. Lett.* **1987**, *58*, 2059–2062.
2. John, S. Strong Localization of Photons in Certain Disordered Dielectric Superlattices. *Phys. Rev. Lett.* **1987**, *58*, 2486–2489.
3. Deubel, M.; Von Freymann, G.; Wegener, M.; Pereira, S.; Busch, K.; Soukoulis, C. M. Direct Laser Writing of Three-Dimensional Photonic-Crystal Templates for Telecommunications. *Nat. Mater.* **2004**, *3*, 444–447.
4. Sun, H. B.; Tanaka, T.; Takada, K.; Kawata, S. Two-Photon Photopolymerization and Diagnosis of Three-Dimensional Microstructures Containing Fluorescent Dyes. *Appl. Phys. Lett.* **2001**, *79*, 1411–1413.
5. Straub, M.; Nguyen, L. H.; Fazlic, A.; Gu, M. Complex-Shaped Three-Dimensional Microstructures and Photonic Crystals Generated in a Polysiloxane Polymer by Two-Photon Microstereolithography. *Opt. Mater.* **2004**, *27*, 359–364.
6. Haske, W.; Chen, V. W.; Hales, J. M.; Dong, W. T.; Barlow, S.; Marder, S. R.; Perry, J. W. 65 nm Feature Sizes using Visible Wavelength 3-D Multiphoton Lithography. *Opt. Express* **2007**, *15*, 3426–3436.
7. Kaneko, K.; Sun, H. B.; Duan, X. M.; Kawata, S. Submicron Diamond-Lattice Photonic Crystals Produced by Two-Photon Laser Nanofabrication. *Appl. Phys. Lett.* **2003**, *83*, 2091–2093.
8. Seet, K. K.; Juodkazis, S.; Jarutis, V.; Misawa, H. Feature-Size Reduction of Photopolymerized Structures by Femtosecond Optical Curing of SU-8. *Appl. Phys. Lett.* **2006**, *89*, 024106−1024106−3.
9. Sun, H. B.; Suwa, T.; Takada, K.; Zaccaria, R. P.; Kim, M. S.; Lee, K. S.; Kawata, S. Shape Precompensation in Two-Photon Laser Nanowriting of Photonic Lattices. *Appl. Phys. Lett.* **2004**, *85*, 3708–3710.
10. Livage, J.; Sanchez, C. Sol-Gel Chemistry. *J. Non-Cryst. Solids* **1992**, *145*, 11–19.
11. Ro, J. C.; Chung, I. J. Sol-Gel Kinetics of Tetraethylorthosilicate (TEOS) in Acid Catalyst. *J. Non-Cryst. Solids* **1989**, *110*, 26–32.
12. Kline, A. A.; Rogers, T. N.; Mullins, M. E.; Cornilsen, B. C.; Sokolov, L. M. Sol−Gel Kinetics for the Synthesis of Multi-Component Glass Materials. *J. Sol−Gel Sci. Technol.* **1994**, *2*, 269–272.
13. Serbin, J.; Egbert, A.; Ostendorf, A.; Chichkov, B. N.; Houbertz, R.; Domann, G.; Schulz, J.; Cronauer, C.; Fröhlich, L.; Popall, M. Femtosecond Laser-Induced Two-Photon Polymerization of Inorganic−Organic Hybrid Materials for Applications in Photonics. *Opt. Lett.* **2003**, *28*, 301–303.
14. Oubaha, M.; Kribich, R. K.; Copperwhite, R.; Etienne, P.; O'Dwyer, K.; MacCraith, B. D. New Organic Inorganic Sol−Gel Material with High Transparency at 1.55 μm. *Opt. Commun.* **2005**, *253*, 346–351.
15. Bhuian, B.; Winfield, R. J.; O'Brien, S.; Crean, G. M. Investigation of the Two-Photon Polymerisation of a Zr-Based Inorganic−Organic Hybrid Material System. *Appl. Surf. Sci.* **2006**, *252*, 4845–4849.
16. Segawa, H.; Yamaguchi, S.; Yamazaki, Y.; Yano, T.; Shibata, S.; Misawa, H. Top-Gathering Pillar Array of Hybrid Organic-Inorganic Material by Means of Self-Organization. *Appl. Phys. A: Mater. Sci. Process.* **2006**, *83*, 447–451.
17. Zhang, H. X.; Lu, D.; Peyghambarian, N.; Fallahi, M.; Luo, J. D.; Chen, B. Q.; Jenl, K.-Y. Electro-Optic Properties of Hybrid Sol-Gel Doped with a Nonlinear Chromophore with Large Hyperpolarizability. *Opt. Lett.* **2005**, *30*, 117–119.
18. Lu, D.; Zhang, H. X.; Fallahi, M. Electro-Optic Modulation in Hybrid Sol-Gel Doped with Disperse Red Chromophore. *Opt. Lett.* **2005**, *30*, 278–280.
19. Saravanamuttu, K.; Blanford, C. F.; Sharp, D. N.; Dedman, E. R.; Turberfield, A. J.; Denning, R. G. Sol−Gel Organic−Inorganic Composites for 3-D Holographic Lithography of Photonic Crystals with Submicron Periodicity. *Chem. Mater.* **2003**, *15*, 2301–2304.
20. Monneret, S.; Huguet-Chantôme, P.; Flory, F. M-Lines Technique: Prism Coupling Measurement and Discussion of Accuracy for Homogeneous Waveguides. *J. Opt. A: Pure Appl. Opt.* **2000**, *2*, 188–195.
21. Sun, H.-B.; Kawata, S. Two-Photon Photopolymerization and 3D Lithographic Microfabrication In *NMR. 3D Analysis. Photopolymerization*; Fatkullin, N., Ed. Springer: Berlin/Heidelberg, 2004; Vol. 170, pp 169−273.
22. Ovsianikov, A.; Passinger, S.; Houbertz, R.; Chichkov, B. N. In *Laser Ablation and its Applications*; Phipps, C. R., Eds.; Springer Series in Optical Sciences 2006; pp 129−167.
23. Serbin, J.; Ovsianikov, A.; Chichkov, B. Fabrication of Woodpile Structures by Two-Photon Polymerization and Investigation of Their Optical Properties. *Opt. Express* **2004**, *12*, 5221–5228.
24. Romanov, S. G.; Maka, T.; Sotomayor Torres, C. M.; Müller, M.; Zentel, R.; Cassagne, D.; Manzanares-Martinez, J.; Jouanin, C. Diffraction of Light from Thin-Film Polymethylmethacrylate Opaline Photonic Crystals. *Phys. Rev. E* **2001**, *63*, 056603-1–056603-5.
25. Romanov, S. G.; Bardosova, M.; Whitehead, D. E.; Povey, I. M.; Pemble, M.; Torres, C. M. S. Erasing Diffraction Orders: Opal *versus* Langmuir−Blodgett Colloidal Crystals. *Appl. Phys. Lett.* **2007**, *90*, 133101-1–133101-3.
26. Lavrinenko, A. V.; Romanov, S. G. Presented at the PECS-VII, Monterey, USA, April 2007.
27. Oubaha, M.; Smaihi, M.; Etienne, P.; Coudray, P.; Moreau, Y. Spectroscopic Characterization of Intrinsic Losses in an Organic−Inorganic Hybrid Waveguide Synthesized by the Sol−Gel Process. *J. Non-Cryst. Solids* **2003**, *318*, 305–313.
28. Jun, Y.; Nagpal, P.; Norris, D. J. Thermally Stable Organic−Inorganic Hybrid Photoresists for Fabrication of Photonic Band Gap Structures with Direct Laser Writing. *Adv. Mater.* **2008**, *20*, 606–610.